

Recent results of Baryon electromagnetic form factors at BESIII

Hua Shi^{a,*} on behalf of the BESIII Collaboration

^a*University of Science and Technology of China, Hefei 230026, People's Republic of China*

E-mail: shih21@mail.ustc.edu.cn

Electromagnetic form factors are fundamental properties of the baryons, which connect to charge, current distributions and provide a crucial testing ground for models of the baryons' internal structure and dynamics. BESIII detector records symmetric e^+e^- collisions in the τ -charm region, which is an ideal platform to study the baryon electromagnetic form factors. There are recent results in BESIII not only for the nucleons, proton and neutron, but also for the hyperons, Λ , Σ and Ξ , as well as the charmed baryon Λ_c .

*The XVIth Quark Confinement and the Hadron Spectrum Conference (QCHSC24)
19-24 August, 2024
Cairns Convention Centre, Cairns, Queensland, Australia*

*Speaker

1. Introduction

Electromagnetic form factors (EMFFs), which parametrize the inner structure of hadrons, are fundamental observables for understanding the strong interaction. EMFFs can be measured in different kinematic regions by (i) lepton elastic scattering for space-like (SL) region of negative q^2 , (ii) annihilation interactions for time-like (TL) region of positive q^2 . For a spin-1/2 baryon (B), the Born differential cross section in the approximation of the one-photon exchange process $e^+e^- \rightarrow B\bar{B}$ is parametrized in terms of electric and magnetic form factors, G_E and G_M , by [1]:

$$\frac{d\sigma_{B\bar{B}}}{d\cos\theta} = \frac{\pi\alpha^2 C\beta}{2q^2} \left((1 + \cos^2\theta)|G_M|^2 + \frac{1}{\tau}|G_E|^2 \sin^2\theta \right), \tau = \frac{q^2}{4m_B^2}, \quad (1)$$

where q^2 is the four-momentum transfer squared, θ is the polar angle in the center-of-mass frame, m_B^2 is the baryon mass and $\beta = \sqrt{1 - 4m_B^2/q^2}$. The Coulomb enhancement factor, C , accounts for the electromagnetic interaction between the outgoing baryons. The effective form factors G_{eff} can be calculated from the total cross section under the assumption of $|G_E| = |G_M|$. According to the optical theorem, TL form factor is in complex form, which leads to transversely polarized baryon even the beams are unpolarized [2, 3]. Thus, a complete knowledge of EMFFs includes the relative phase $\Delta\Phi$ between G_E and G_M . The nonzero $\Delta\Phi$ shows a dependence of the polarization on the scattering angle [4, 5]:

$$p_y = -\frac{\sin 2\theta \text{Im}[G_E \cdot G_M^*]/\sqrt{\tau}}{\frac{|G_E|^2 \sin^2\theta}{\tau} + |G_M|^2(1 + \cos^2\theta)}. \quad (2)$$

In experiment, the TL form factors can be measured by two methods, (i) energy scan method at discrete center-of-mass (c.m.) energies (\sqrt{s}), leaving gaps without information, with the advantage of lower background and good energy resolution; (ii) initial state radiation (ISR) method at a fixed c.m. energy with the advantages of continuous measurements, from threshold to \sqrt{s} , and systematic uncertainty study in a coherent way, but under the limitation of data luminosity and higher background. These methods complement each other and provide comprehensive data for the study of baryon EMFFs.

BESIII has collected large data samples in the τ -charm region. Both energy scan method and ISR method can be used to do precise measurements to help understand the properties of baryons.

2. EMFFs of nucleons

Proton and neutron are the fundamental building blocks of the atomic nucleus. Their EMFFs measurements are straightforward to describe the complex internal structure, leading to the understanding of the quantum chromodynamics (QCD) at low momentum transfer.

Born cross section ($\sigma_{p\bar{p}}$), $|G_{\text{eff}}|$ and form factor ratio $|G_E/G_M|$ of proton have been measured with high accuracy by using two techniques. Energy scan method is used in two datasets, c.m. energies from 2.2324 to 3.6710 GeV with the luminosity of 156.9 pb^{-1} [6] and 2.0000 to 3.0800 GeV with the luminosity of 688.5 pb^{-1} [7]. According to the angular distributions, $|G_E/G_M|$ is determined with the precision of 3.5% at $\sqrt{s} = 2.1250 \text{ GeV}$. What's more, $|G_M|$ is measured for the first time over a wide range of energies with uncertainties of 1.6% to 3.9% and $|G_E|$ is obtained for

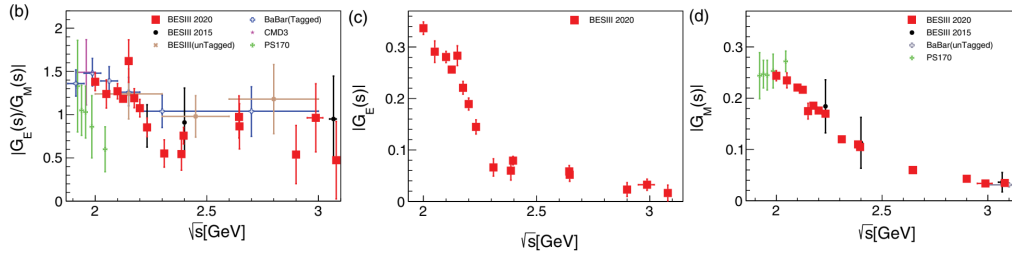


Figure 1: Form factor ratio $|G_E/G_M|$, $|G_M|$ and $|G_E|$ of proton as a function of c.m. energy.

the first time, which are shown in Fig. 1. Using several data sets with a total luminosity of 7.5 fb^{-1} at $\sqrt{s} = 3.773\text{--}4.600 \text{ GeV}$, the cross sections and $|G_{\text{eff}}|$ are measured from $p\bar{p}$ threshold to $3.0 \text{ GeV}/c^2$ or from 2.0 to $3.8 \text{ GeV}/c^2$ through the ISR process, where ISR photon emits at large angle (LA) [8] or small angle (SA) [9], respectively. Among them, BESIII results are consistent with the previous measurements shown in Fig. 2. The most precise ones are obtained at $\sqrt{s} = 2.1250 \text{ GeV}$ with $\delta\sigma_{p\bar{p}} \sim 3.0\%$ and $\delta|G_{\text{eff}}| \sim 1.5\%$. Periodic oscillations are found at the proton effective form

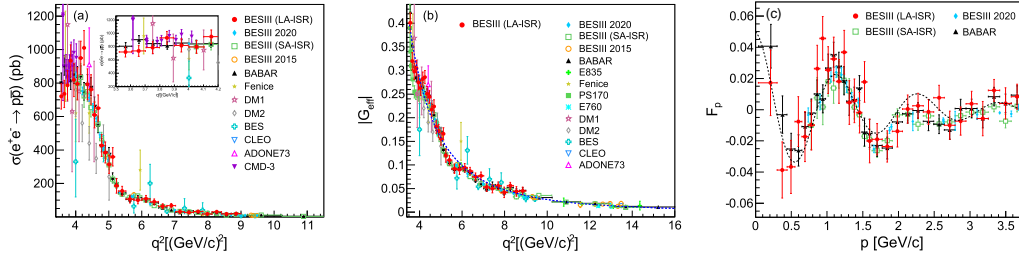


Figure 2: Born cross sections for the process $e^+e^- \rightarrow p\bar{p}$ (a), $|G_{\text{eff}}|$ of the proton (b) and the effective form factor after subtraction of the smooth function dependent on the relative momentum p (c) at BESIII, together with the results from previous experiments.

factor as a function of p after subtraction of the smooth function proposed in Ref. [10]:

$$|G_{\text{eff}}| = \frac{\mathcal{A}}{(1 + q^2/m_a^2)(1 - q^2/q_0^2)^2}, \quad q_0^2 = 0.71 \text{ GeV}/c^2. \quad (3)$$

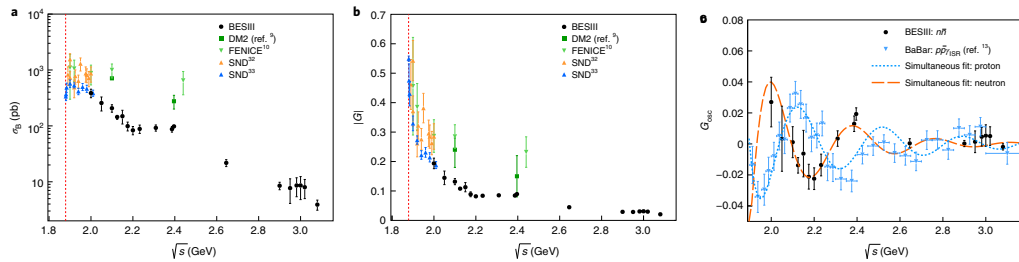


Figure 3: Born cross sections for the process $e^+e^- \rightarrow n\bar{n}$ (a), corresponding $|G_{\text{eff}}|$ of neutron (b) and the form factor deviation from the dipole law (c) with respect to the c.m. energy.

Neutron and anti-neutron pairs produced in e^+e^- annihilation for \sqrt{s} between 2.00 and 3.08 GeV is studied by BESIII, where the datasets represent the first high-luminosity off-resonance energy

scan. A precise measurement of Born cross sections and $|G_{\text{eff}}|$ are achieved, which are shown in Fig. 3. For $\sqrt{s} = 2.00, 2.10$ and 2.40 GeV, the precision is improved over previous measurements from the FENICE and DM2 experiments by factors of about three, two and six, respectively [11]. Oscillation of reduced- $|G_{\text{eff}}|$ is observed in neutron with a phase orthogonal to the proton. Values of $|G_E|$, $|G_M|$ and $|G_E/G_M|$ are extracted at five c.m. energy intervals in the TL region. Compared with the FENICE results [12], the results for $|G_M|$ from BESIII [13] are smaller by a factor of $\sim 2 - 3$ in the range of $\sqrt{s} = 2.00 - 2.50$ GeV, as shown in Fig. 4. The measured $|G_E|$ and $|G_M|$ can be used to test various models, such as a parametrization obtained from the pQCD, a modified dipole model (MD), a vector meson dominance model (VMD) and a model based on dispersion relations (DR), to provide a more comprehensive picture of the neutron structure. DR model gives the best consistency.

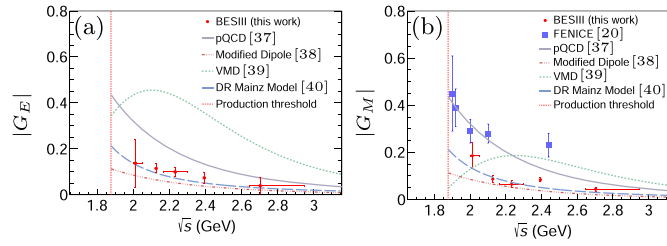


Figure 4: Electric (a) and Magnetic (b) form factors of neutron as a function of c.m. energy together with FENICE results and four different parametrizations.

3. EMFFs of hyperons

Compared to nucleons, it is difficult to study EMFFs of hyperons in SL due to the difficulty in stable and high-quality hyperon beams. In e^+e^- machines, hyperons pair can be produced in the annihilation process above their production threshold. The cross section can be obtained very close to threshold with finite phase space of final states. With hyperon weak decay to baryon and pseudo-scalar meson, the polarization of hyperon can be measured by the angular distribution, so does the relative phase between G_E and G_M .

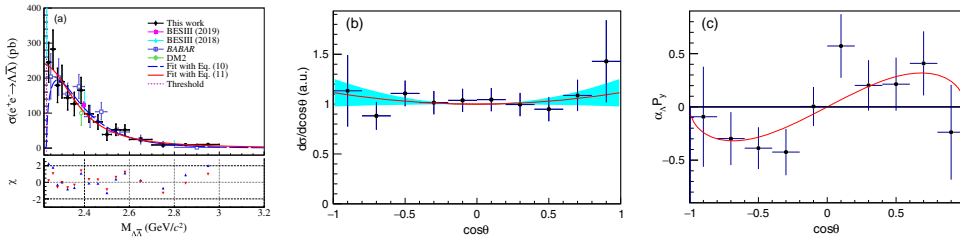


Figure 5: Cross section for the process $e^+e^- \rightarrow \Lambda \bar{\Lambda}$ (a), together with the results from previous works. The accepted corrected Λ scattering angle distribution (b) and the product of α_Λ and Λ polarization p_y as a function of the scattering angle (c).

Cross sections of $e^+e^- \rightarrow \Lambda \bar{\Lambda}$ are measured at BESIII by two methods near threshold. Energy scan method is used at $\sqrt{s} = 2.2324$ (1 MeV above threshold), 2.4000, 2.8000 and 3.0800 GeV [14].

ISR method is used at $\sqrt{s} = 3.773\text{--}4.258\text{ GeV}$ with a total luminosity of 11.9 fb^{-1} and cross sections from threshold to $3.0\text{ GeV}/c^2$ are obtained [15]. Nonzero cross section near threshold is observed shown in Fig. 5, which is consistent with BaBar results [16]. A complete measurement of Λ EMFFs is studied at 2.3960 GeV , 66.9 pb^{-1} . An event of the reaction $e^+e^- \rightarrow \Lambda(\rightarrow p\pi^-)\bar{\Lambda}(\rightarrow \bar{p}\pi^+)$ is formalized by joint angular distribution:

$$W(\xi) = \mathcal{T}_0 + \eta\mathcal{T}_5 - \alpha_\Lambda^2 \left[\mathcal{T}_1 + \sqrt{1 - \eta^2} \cos(\Delta\Phi)\mathcal{T}_2 + \eta\mathcal{T}_6 \right] + \alpha_\Lambda \sqrt{1 - \eta^2} \sin(\Delta\Phi)(\mathcal{T}_3 - \mathcal{T}_4), \quad (4)$$

which contains three parts, unpolarized, correlated and polarized part. Using this fully differential angular description of the final state particles, both $|G_E/G_M|$, equal to $0.96 \pm 0.14 \pm 0.02$, and relative phase, $\Delta\Phi = 37^\circ \pm 12^\circ \pm 6^\circ$, are extracted [17], shown in Fig. 5. The nonzero relative phase confirms the complex form of EMFFs.

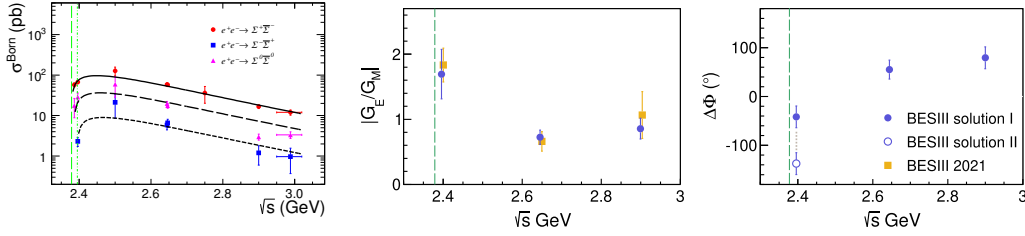


Figure 6: Cross section for the process $e^+e^- \rightarrow \Sigma^\pm\bar{\Sigma}^\mp/\Sigma^0\bar{\Sigma}^0$ (left), results for $|G_E/G_M|$ (middle) and the relative phase $\Delta\Phi$ (right) of Σ^+ as a function of c.m. energy

For Σ hyperons, Born cross sections of isospin triplets, Σ^+ , Σ^- and Σ^0 , are measured from threshold to $3.02\text{ GeV}/c^2$ via energy scan method [18, 19], shown in Fig. 6. The cross sections can be well described by pQCD-motivated functions. An asymmetry in cross section is observed, $9.7 \pm 1.3 : 3.3 \pm 0.7 : 1$, which may relate with valence quark. Via ISR technique using data with an integrated luminosity of 11.9 fb^{-1} , collected at $\sqrt{s} = 3.773\text{--}4.258\text{ GeV}$, the process $e^+e^- \rightarrow \Sigma^+\bar{\Sigma}^-$ is studied from threshold to $3.04\text{ GeV}/c^2$ [20]. No significant threshold effect is observed. A complete measurement of Σ^+ EMFFs is studied at $\sqrt{s} = 2.3960, 2.6454$ and 2.9000 GeV in Fig. 6, with the polarization significance of $2.2\sigma, 3.6\sigma$ and 4.1σ , respectively [21]. For the first time, the phase of the hyperon electromagnetic form factors is explored in a wide range of four-momentum transfer.

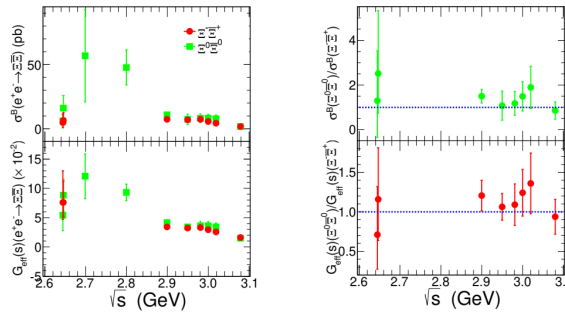


Figure 7: Cross sections and $|G_{\text{eff}}|$ for Ξ^- and Ξ^0 (left) and ratio of them between Ξ doublets (right).

Born cross sections of Ξ isospin doublets, Ξ^- and Ξ^0 , are measured from threshold to $3.0800 \text{ GeV}/c^2$ [22, 23]. No significant threshold effect is observed, shown in Fig. 7. The ratio of Born cross sections and $|G_{\text{eff}}|$ for both modes is within 1σ of the expectation of isospin symmetry.

As the charm analog of proton, the Λ_c hadron can shed new light on baryon structure. Measurements of cross section and $|G_E/G_M|$ with high accuracy are performed at $\sqrt{s} = 4.5745 - 4.9509 \text{ GeV}$ [24, 25]. Enhanced cross section near threshold is observed, $236 \pm 11 \pm 46 \text{ pb}$ at $\sqrt{s} = 4.5745 \text{ GeV}$, 1.6 MeV above threshold. Flat behavior around 4.63 GeV may indicate no enhancement around the $Y(4630)$ resonance shown in Fig. 8, which is different from Belle results [26]. No oscillatory behavior is discerned in $|G_{\text{eff}}|$ Spectrum of Λ_c^+ , in contrast to the case for proton and neutron. An oscillation behavior is observed in the energy dependence of $|G_E/G_M|$.

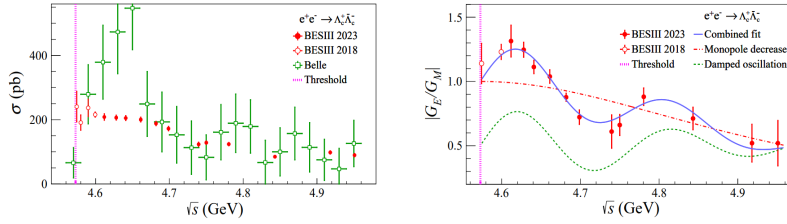


Figure 8: Cross section for the process $e^+e^- \rightarrow \Lambda_c^+ \bar{\Lambda}_c^-$ (left), together with the results from Belle and the $|G_E/G_M|$ of Λ_c^+ (right) as a function of c.m. energy.

4. Summary

There are fruitful physics results of baryon EMFFs obtained from e^+e^- colliders, vis energy scan and ISR techniques, part of which are summarized in Fig. 9. Conventional parametrization of EMFFs is facing challenge from experimental observations, like threshold enhancement, oscillation behavior in reduced form factors and $|G_E/G_M|$. Using the property of short life and weak decay of hyperons, relative phase of EMFFs gives rise to polarization of final baryons, and play an important role in distinguishing various theoretical models. More results from BESIII are on the way.

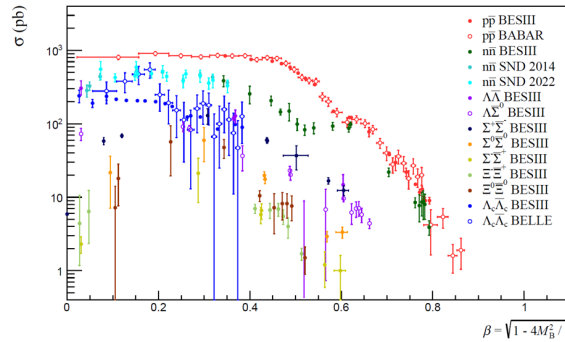


Figure 9: Summary of the cross sections of baryons updated from Ref. [27].

References

- [1] N. Cabibbo and R. Gatto, *Electron Positron Colliding Beam Experiments*, *Phys. Rev.* **124** (1961) 1577.
- [2] E. Tomasi-Gustafsson, F. Lacroix, C. Duterte and G.I. Gakh, *Nucleon electromagnetic form-factors and polarization observables in space-like and time-like regions*, *Eur. Phys. J. A* **24** (2005) 419 [[nucl-th/0503001](#)].
- [3] A. Denig and G. Salme, *Nucleon Electromagnetic Form Factors in the Timelike Region*, *Prog. Part. Nucl. Phys.* **68** (2013) 113 [[1210.4689](#)].
- [4] A.Z. Dubnickova, S. Dubnicka and M.P. Rekalo, *Investigation of the nucleon electromagnetic structure by polarization effects in $e^+e^- \rightarrow N \text{ anti-}N$ processes*, *Nuovo Cim. A* **109** (1996) 241.
- [5] G. Fäldt and A. Kupsc, *Hadronic structure functions in the $e^+e^- \rightarrow \bar{\Lambda}\Lambda$ reaction*, *Phys. Lett. B* **772** (2017) 16 [[1702.07288](#)].
- [6] BESIII collaboration, *Measurement of the proton form factor by studying $e^+e^- \rightarrow p\bar{p}$* , *Phys. Rev. D* **91** (2015) 112004.
- [7] BESIII collaboration, *Measurement of proton electromagnetic form factors in $e^+e^- \rightarrow p\bar{p}$ in the energy region 2.00 - 3.08 GeV*, *Phys. Rev. Lett.* **124** (2020) 042001.
- [8] BESIII collaboration, *Measurement of proton electromagnetic form factors in the time-like region using initial state radiation at BESIII*, *Phys. Lett. B* **817** (2021) 136328.
- [9] BESIII collaboration, *Study of the process $e^+e^- \rightarrow p\bar{p}$ via initial state radiation at BESIII*, *Phys. Rev. D* **99** (2019) 092002.
- [10] E. Tomasi-Gustafsson and M.P. Rekalo, *Search for evidence of asymptotic regime of nucleon electromagnetic form-factors from a compared analysis in space- and time - like regions*, *Phys. Lett. B* **504** (2001) 291.
- [11] BESIII collaboration, *Oscillating features in the electromagnetic structure of the neutron*, *Nature Phys.* **17** (2021) 1200.
- [12] A. Antonelli et al., *The first measurement of the neutron electromagnetic form-factors in the timelike region*, *Nucl. Phys. B* **517** (1998) 3.
- [13] BESIII collaboration, *Measurements of the Electric and Magnetic Form Factors of the Neutron for Timelike Momentum Transfer*, *Phys. Rev. Lett.* **130** (2023) 151905.
- [14] BESIII collaboration, *Observation of a cross-section enhancement near mass threshold in $e^+e^- \rightarrow \Lambda\bar{\Lambda}$* , *Phys. Rev. D* **97** (2018) 032013.
- [15] BESIII collaboration, *Measurement of the $e^+e^- \rightarrow \Lambda\bar{\Lambda}$ cross section from threshold to 3.00 GeV using events with initial-state radiation*, *Phys. Rev. D* **107** (2023) 072005.

- [16] BABAR collaboration, *Study of $e^+e^- \rightarrow \Lambda\bar{\Lambda}, \Lambda\bar{\Sigma}^0, \Sigma^0\bar{\Sigma}^0$ using initial state radiation with BABAR*, *Phys. Rev. D* **76** (2007) 092006.
- [17] BESIII collaboration, *Complete Measurement of the Λ Electromagnetic Form Factors*, *Phys. Rev. Lett.* **123** (2019) 122003.
- [18] BESIII collaboration, *Measurements of Σ^+ and Σ^- time-like electromagnetic form factors for center-of-mass energies from 2.3864 to 3.0200 GeV*, *Phys. Lett. B* **814** (2021) 136110.
- [19] BESIII collaboration, *Measurement of the $e^+e^- \rightarrow \Sigma^0\bar{\Sigma}^0$ cross sections at center-of-mass energies from 2.3864 to 3.0200 GeV*, *Phys. Lett. B* **831** (2022) 137187.
- [20] BESIII collaboration, *Measurements of Σ electromagnetic form factors in the timelike region using the untagged initial-state radiation technique*, *Phys. Rev. D* **109** (2024) 034029.
- [21] BESIII collaboration, *Determination of the Σ^+ Timelike Electromagnetic Form Factors*, *Phys. Rev. Lett.* **132** (2024) 081904.
- [22] BESIII collaboration, *Measurement of cross section for $e^+e^- \rightarrow \Xi^-\bar{\Xi}^+$ near threshold at BESIII*, *Phys. Rev. D* **103** (2021) 012005.
- [23] BESIII collaboration, *Measurement of cross section for $e^+e^- \rightarrow \Xi^0\bar{\Xi}^0$ near threshold*, *Phys. Lett. B* **820** (2021) 136557.
- [24] BESIII collaboration, *Precision measurement of the $e^+e^- \rightarrow \Lambda_c^+\bar{\Lambda}_c^-$ cross section near threshold*, *Phys. Rev. Lett.* **120** (2018) 132001.
- [25] BESIII collaboration, *Measurement of Energy-Dependent Pair-Production Cross Section and Electromagnetic Form Factors of a Charmed Baryon*, *Phys. Rev. Lett.* **131** (2023) 191901.
- [26] BELLE collaboration, *Observation of a near-threshold enhancement in the $e^+e^- \rightarrow \Lambda_{b(c)}^+\Lambda_{b(c)}^-$ cross section using initial-state radiation*, *Phys. Rev. Lett.* **101** (2008) 172001.
- [27] G. Huang and R.B. Ferrolì, *Probing the internal structure of baryons*, *Natl. Sci. Rev.* **8** (2021) nwab187.